Journal of Alloys and Compounds 639 (2015) 139–144

Contents lists available at ScienceDirect

Journal of Alloys and Compounds

journal homepage: www.elsevier.com/locate/jalcom

Magnetization and ESR studies of $La_{0.67}(Ca_{1-x}Mg_x)_{0.33}MnO_3$ systems

A. Sendil Kumar [a,*], Ravinder Reddy K [b], Anil K. Bhatnagar [a,b,*]

[a] School of Physics, University of Hyderabad, Hyderabad, Telangana, 500 046, India
[b] School of Engineering Sciences & Technology, University of Hyderabad, Hyderabad, Telangana, 500 046, India

ARTICLE INFO

Article history:
Received 3 October 2014
Received in revised form 7 February 2015
Accepted 4 March 2015
Available online 10 March 2015

Keywords:
Manganites
ESR
Jahn–Teller distortion
Griffiths phase

ABSTRACT

Magnetization studies and line shape analysis on Electron Spin Resonance (ESR) spectra of $La_{0.67}(Ca_{1-x}Mg_x)_{0.33}MnO_3$ are carried out. In paramagnetic phase well above T_c, the ESR spectra are single Lorentzian but below and near $T^*_{\Delta HPP}$, ($T^*_{\Delta HPP}$ is temperature at which line width is minimum) inhomogeneous broadening with asymmetry in the signal is observed due to phase separation. The resonance field below $T^*_{\Delta HPP}$ decreases with decreasing temperature. Above T_c the intensity of the ESR spectra obeys the thermally activated model (Arrhenius behavior). Substitution of Mg weakens the ferromagnetic interaction and evolution of change in lineshape near T_c is an evidence of Griffiths phase (coexistence of paramagnetic and ferromagnetic) in Mg doped LCMO system.

1. Introduction

Colossal magnetoresistance (CMR) materials have been studied for last three decades due to rich magnetic phase diagram. The structural, magnetic and transport properties of manganites $La_{1-x}M_xMnO_3$ ($M = Ca^{2+}$, Sr^{2+}, Ba^{2+}) depend on MnO_6 octahedra and variation in La site doping. For $La_{1-x}Ca_xMnO_3$, two extreme compounds with $x = 0$ and $x = 1$ are $LaMnO_3$ and $CaMnO_3$. Stoichiometric $LaMnO_3$ has orthorhombic crystal structure and is an antiferromagnetic insulator with Néel temperature T_N of 140 K [1] while $CaMnO_3$ is a G-type antiferromagnet insulator with T_N of 110 K [2]. If the tolerance factor [3] deviates from ideal unity value then there are two types of distortions associated with the orbital degeneracy in 3d-e_g level, namely, static Jahn–Teller (JT) distortion and dynamic JT distortion. When the system structurally changes from orthorhombic to rhombohedral only dynamic JT is expected. This distortion in manganites influences electrostatic energies in the lattice which plays a role in magnetic properties. Concentration or amount of doping in La site alters the ratio of Mn^{3+} to Mn^{4+}, distances of Mn–O bond and Mn–O–Mn bond angles of MnO_6 octahedral network. Substituting optimal amount of selective cation doping in La site can alter the different interaction energies like charge transfer energy, on-site Coulomb energy, exchange energy and crystal field energy in comparable values which play vital role in charge, spin and lattice degrees of freedom. Doping M in the range of $0.2 < M < 0.5$ makes $La_{1-x}M_xMnO_3$ shift from a paramagnetic insulator to a ferromagnetic metal [4]. The magnetic phase diagram of different amount of Ca doped $LaMnO_3$ is already available in the literature [5–7]. Researchers are much interested in particular value of hole doped $La_{0.67}Ca_{0.33}MnO_3$ system due to its phase transition from antiferromagnetic to ferromagnetic ordering with Curie temperature close to 250 K and in optimum amount of Sr doped system $La_{0.67}Sr_{0.33}MnO_3$ which are ferromagnetic-metallic [8] and when depositing a heterostructure with $YBa_2Cu_3O_7$–$La_{0.67}Sr_{0.33}MnO_3$–$YBa_2Cu_3O_7$ it shows proximity effect [9,10]. The observed ferromagnetism in these compounds is explained by Zener's Double Exchange (DE) mechanism [10] but the recent theoretical and experimental results reveal that the Double Exchange is not sufficient to explain all the observed physical properties of this composition and strong electron–lattice coupling must be taken into account [11,12]. The origin for inducing electron–lattice coupling in manganites is associated with the dynamic J–T. Other compositions of $La_{1-x}M_xMnO_3$ contain both ferromagnetic and antiferromagnetic components. This paper reports magnetization, AC Susceptibility (ACS) and detailed line shape analysis of the Electron Spin Resonance spectra of effect of B site doping with a non-magnetic Mg in $(La_{0.67}Ca_{0.33})MnO_3$ and some preliminary results have been reported earlier [13].

2. Experimental details

Manganite $La_{0.67}(Ca_{1-x}Mg_x)_{0.33}MnO_3$ samples, with $x = 0$, 0.1, 0.2, 0.3, 0.4 and 0.5, were prepared through the conventional solid state reaction route. Required molar ratio of high purity precursors La_2O_3 (99.99%), $CaCO_3$ (99.9%), $MnCO_3$ (99.9%) and MgO (99.9%) were taken, mixed homogeneously and ground using agate mortar for about one hour. The mixture is then calcined first at 1200 °C for 12 h and then at 1300 °C for 24 h. After calcination, the resulting powder is pressed

* Corresponding authors.
E-mail address: sendilphy@gmail.com (A. Sendil Kumar).

http://dx.doi.org/10.1016/j.jallcom.2015.03.028
0925-8388/

into cylindrical disk pellets with an applied pressure of 300 MPa using hydraulic press and sintered at 1400 °C for 12–24 h in alumina crucibles. Hereafter samples with $x = 0, 0.1, \ldots, 0.5$ will be referred as M0, M1, ...M5, respectively. The sintered pellets were crushed into powder and powder X-ray diffraction pattern were recorded using a Bruker D8 Advance X-ray diffractometer with Cu Kα radiation of wavelength 1.5406 Å. The XRD patterns were indexed and matches well with PCPDF No. 49-0416 as shown in Fig. 1. From the XRD patterns we conclude that all the samples belong to the orthorhombic crystal structure with Pnma space group. Microstructure of each sample is studied with a FE-SEM (Carl-Zeiss) using the powder ground from the sintered pellet and particle size distributions are found to be in microns as shown in Fig. 2.

3. Results and discussion

3.1. Magnetization and AC Susceptibility

Magnetization and AC Susceptibility are carried out using a PPMS-6000 (Quantum Design) equipment. The VSM option is used for magnetization measurements with a resolution of 10^{-6} emu. The ACMS option is used as an AC susceptometer. The drive coil in the ACMS can generate alternating fields up to ±10 Oe in a frequency range of 10 Hz–10 kHz. ESR spectra are recorded using JEOL (JES-FA200) ESR Spectrometer operating at the standard X-band frequency ($\nu = 9.16$ GHz). Besides the electromagnet in the ESR, the instrument is equipped with a pair of secondary coils and a sweep generator. The coils are used to generate an oscillating magnetic field of a maximum amplitude 5 kOe and frequency of 110 kHz. The first derivative dP/dH of the power absorption P is recorded as a function of applied field H in the range 0–8 kOe.

Temperature dependent magnetization (M–T) measurements are carried out using PPMS-VSM (QD). 10 kOe field cooled magnetization measurements were recorded from 5 K to 300 K which are shown in Fig. 3. All the samples M0 to M5 show phase transition from paramagnetic to ferromagnetic while cooling. Samples from M0 to M3 show sharp transition where M4 and M5 exhibit broader transition. The inflection point from first derivative of M–T data with respect to temperature is closely matches with T_c of each sample and is shown in Fig. 4. This T_c value matches well with the peak temperature in the ACS data. Curie temperature (T_c) of M0 ($La_{0.67}Ca_{0.33}MnO_3$, (the parent compound in this series) is close to 267 K and is in good agreement with the literature value [3]. With increase in concentration of Mg, T_c and magnetization decreases. The observed ferromagnetism in this series is due to interplay between the Double Exchange (DE) and the super exchange (SE) interactions. In the $LaMnO_3$ system, Mn exists in 3+ valence state with electronic configuration of $t_{2g}^3 e_g^1$ having half filled e_g orbital. According to Goodenough–Kanamori (GK) first rule, whenever two half filled magnetic cations overlap with an anion (oxygen) p orbital, it favors antiferromagnetic interaction (SE). When Ca or another divalent substitution is done in $LaMnO_3$, it results in mixed valence state of Mn in 3+ and 4+. Mn has electronic configuration of $t_{2g}^3 e_g^0$ in 4+ valence state. Whenever a situation of mixed valence state of Mn exists then more than one type of interactions are possible. According to third GK rule, whenever half filled magnetic cation (Mn^{3+}, e_g^1) and an empty magnetic cation (Mn^{4+}, e_g^0) overlap through p orbital of anion then the interaction is ferromagnetic. The DE also favors ferromagnetic interaction when a same magnetic cation (Mn) atoms with different valence states overlaps with oxygen. Optimally hole doped $La_{0.67}Ca_{0.33}MnO_3$, the parent compound of this series, is ferromagnetic. In $La_{0.67}(Ca_{1-x}Mg_x)_{0.33}MnO_3$ series, we expect that there will be a gradual change in Mn^{3+}–Mn^{3+} and Mn^{3+}–Mn^{4+} distances and bond angle which will alter the strength of DE and SE interactions [14]. In the present series with $x = 0$ to $x = 0.3$ (M0 to M3) the ferromagnetic transition is sharper than that in $x = 0.4$ and 0.5 (M4 and M5). The observed ferromagnetic interaction is due to induced dynamic JT polaron [15]. Temperature dependence of Susceptibility obeys Curie–Weiss law above T_c and the effective magnetic moments are calculated using $\sqrt{7.99 * C}$ [16], where C is Curie's constant (drawn from $1/\chi$ against T plot). The calculated effective moment values, calculated from this relation, are given in Table 1. The ACS measurement is carried out at 71 Hz frequency with field amplitude of 5 Oe. The observed feature in ACS resembles with those observed in dc magnetization data. The Curie temperature observed from dc magnetization matches closely with the peak temperature in the ACS data seem to be ferromagnetic order which is shown in Fig. 5.

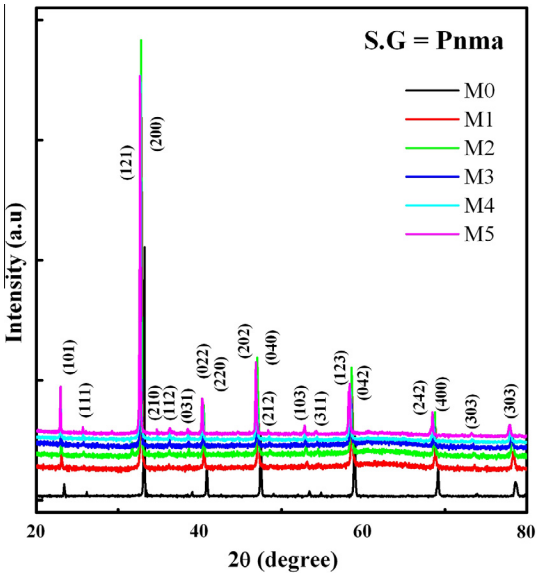

Fig. 1. Powder XRD pattern recorded using Cu Kα of wavelength 1.5406 Å for M0 to M5 and indexed with space group Pnma.

3.2. Line shape analysis on ESR data

Temperature dependent ESR spectra (field vs first derivative of microwave power absorption) from123 K to 313 K are recorded with a JEOL-ESR spectrometer operating at the X band frequency of 9.2 GHz. A strong ESR signal with a line shape of Lorentzian is observed over the temperature range of the paramagnetic region for each sample. Same amount of mass is taken for all the samples for the ESR measurements. The observed ESR signals are very intense and are single Lorentzian above T_c. The ESR linewidth ($\Delta H_{PP}(T)$) passes through a minimum and below T_c it increases drastically. Two different kinds of paramagnetic centres, namely, Mn^{3+} (d^4, $S = 2$) and Mn^{4+} (d^3, $S = 3/2$) form an extended lattice and are subjected to the exchange and dipolar interactions. The fourth electron of Mn^{3+} is J–T active and undergoes split in e_g orbital and it is not stationary. It hops between Mn^{3+} and Mn^{4+} sites through Jahn–Teller polaron which is responsible for the ESR spectra [17].

As mentioned above, each ESR spectrum has a single line with Lorentzian shape above T_c. The line broadening takes place near T_c and is found to be inhomogeneous and the asymmetry also starts developing. The lineshape is entirely changed well below T_c due to local molecular field and the inhomogeneity in the sample. Even in single crystals of manganites with high chemical purity, different electronic and magnetic properties coexist at different parts of the sample. This is called phase separation (PS) and it occurs at various length scales ranging from sub-nanometers to few microns sometimes. Manganites are intrinsically inhomogeneous and observed inhomogeneous broadening below T_c is attributed to PS and till now CMR is believed due to PS [18].